Results in Chemistry 9 (2024) 101614

Contents lists available at ScienceDirect

Results in Chemistry

journal homepage: www.sciencedirect.com/journal/results-in-chemistry

Silver@copper-polyaniline nanotubes: Synthesis, characterization and biosensor analytical study

Mohamed J. Saadh [a], H.N.K. AL-Salman [b], Hussein H. Hussein [b], Zaid H. Mahmoud [c,*], Hamza Hameed Jasim [d], Zahraa hassan Ward [e], Mahmood Hasen shuhata Alubiady [f], Ahmed Muzahem Al-Ani [g], Sally Salih Jumaa [h], Hamidreza Sayadi [i], Ehsan Kianfar [j,*]

[a] Faculty of Pharmacy, Middle East University, Amman 11831, Jordan
[b] Pharmaceutical Chemistry Department, College of Pharmacy, University of Basrah, Iraq
[c] Department of Chemistry, College of Sciences, University of Diyala, Iraq
[d] Department of Medical Instrumentation Engineering Techniques, Imam Ja'afar Al-Sadiq University, Iraq
[e] Department of Medical Engineering, Mazaya University College, Iraq
[f] Department of Medical Engineering, Al-Hadi University College, Baghdad 10011, Iraq
[g] Department of Medical Engineering, Al-Nisour University College, Baghdad, Iraq
[h] Department of Medical Engineering, National University of Science and Technology, Dhi Qar, Iraq
[i] Young Researchers and Elite Club, Gachsaran Branch, Islamic Azad University, Gachsaran, Iran
[j] Department of Chemical Engineering, Faculty Shahrood branch, Shahrood branch, Shahrood, Iran

ARTICLE INFO

Keywords:
Biosensor
Bimetallic
DPV
Cyclic voltammetry
Nanotube
Bimetallic nanoparticles

ABSTRACT

We introduce silver-copper nanoparticles incorporated into polyaniline (PANI) nanotubes using a straightforward and efficient reduction process. In this regard, PANI nanotubes with amine groups were fabricated through oxidation polymerization, followed by the attachment of Ag and Cu precursors to enable the synthesis of Ag-Cu bimetallic nanoparticles (NPs) on the pre-formed PANI nanotubes with the use of hydrazine as a reducing agent. The structural characterization of the synthesized NPs was investigated by UV–Vis spectrophotometer (UV–Vis), Dark-field emission, (EDX), X-ray diffraction (XRD) and field emission (FESEM), while the electrochemical properties were estimated by (CV) and differential pulse voltammetry (DPV). The findings indicated that the Ag-Cu NPs were present in the nanoscale range, well-dispersed, and attached to the surface of PANI nanotubes. Electrochemical investigations revealed that the Ag-Cu@PANI nanotube electrode demonstrated efficient electrooxidation of dopamine and hydroquinone without any interfering reactions, suggesting its potential use as an electrochemical biosensor for simultaneous detection of dopamine and hydroquinone. The proposed NPs-based biosensor was connected to concurrently identify dopamine and hydroquinone, illustrating moo distinguish Confinements of 0.46 μM for dopamine and 0.23 mM for hydroquinone, separately. Additionally, the manufactured sensor identified on a wide direct run the dopamine (5–25 μM), and hydroquinone (0.5–2.5 mM). Alongside these promising comes about, the Ag-Cu@PANI nanotube actualized great solidness and reproducibility, making it a favorable stage for electrochemical biosensing of dopamine and hydroquinone.

1. Introduction

Dopamine (DA) and hydroquinone (HQ) are two well-known materials with significant biomedical applications [1]. Hydroquinone could be a phenolic compound show broadly and has favorable redox characteristics [2]. It postures a critical natural and wellbeing hazard due to its moo biodegradability and tall harmfulness [3]. Its expansion in pharmaceuticals, cosmetics and the human diet exacerbates ecological defilement and is dangerous to human health [4]. Administrative bodies such as the EU and EPA have recognized hydroquinone as an essential poison, and China has built up a satisfactory emission level of 0.5 mg/mL for this substance. Within the field of medication, dopamine serves as a significant neurotransmitter included in different physiological forms, counting discernment and feeling. Unsettling influences in dopamine levels are embroiled in various therapeutic conditions, such as anorexia and schizophrenia [5]. Untimely revelation can altogether

* Corresponding authors.
E-mail addresses: zaidhameed_91@yahoo.com (Z.H. Mahmoud), ehsan_kianfar2010@yahoo.com, ehsankianfar775@gmail.com (E. Kianfar).

https://doi.org/10.1016/j.rechem.2024.101614
Received 2 April 2024; Accepted 23 June 2024
Available online 26 June 2024

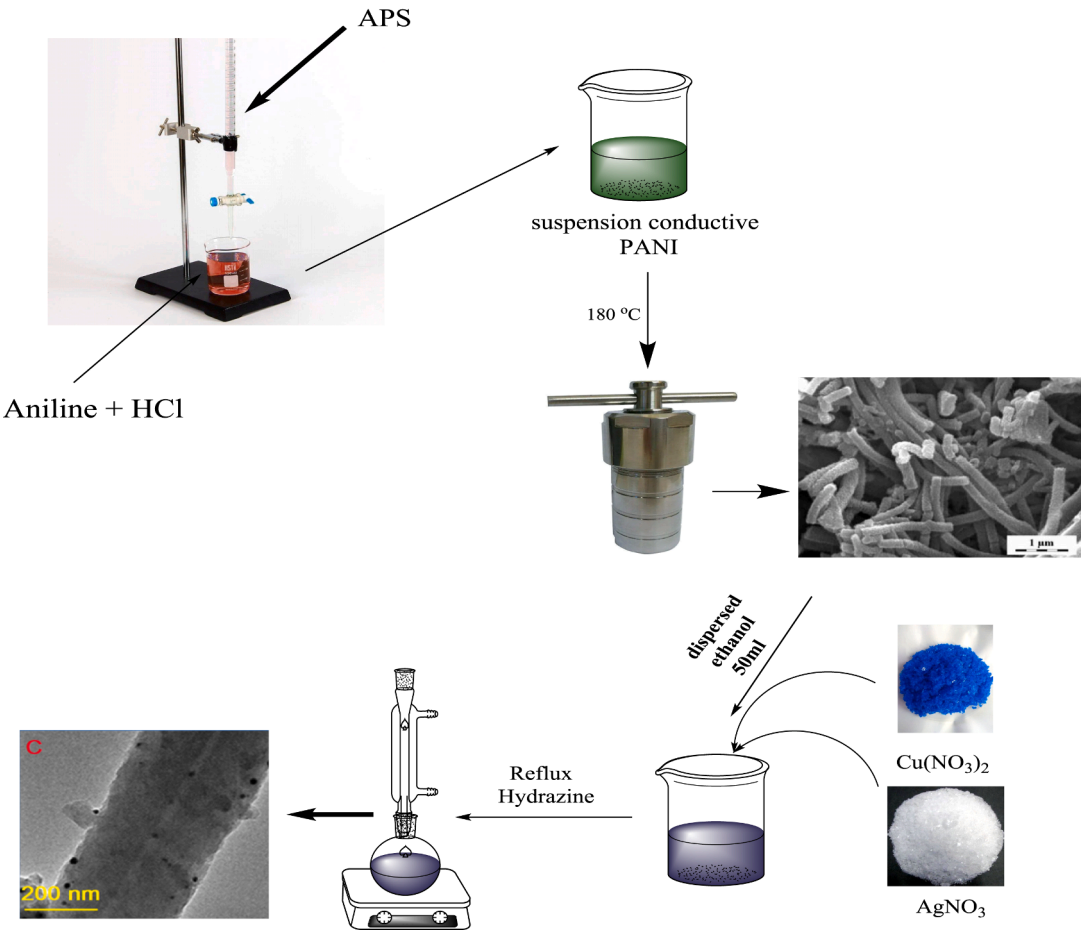

Fig. 1. Producer of steps Ag-Cu@PANI nanotubes.

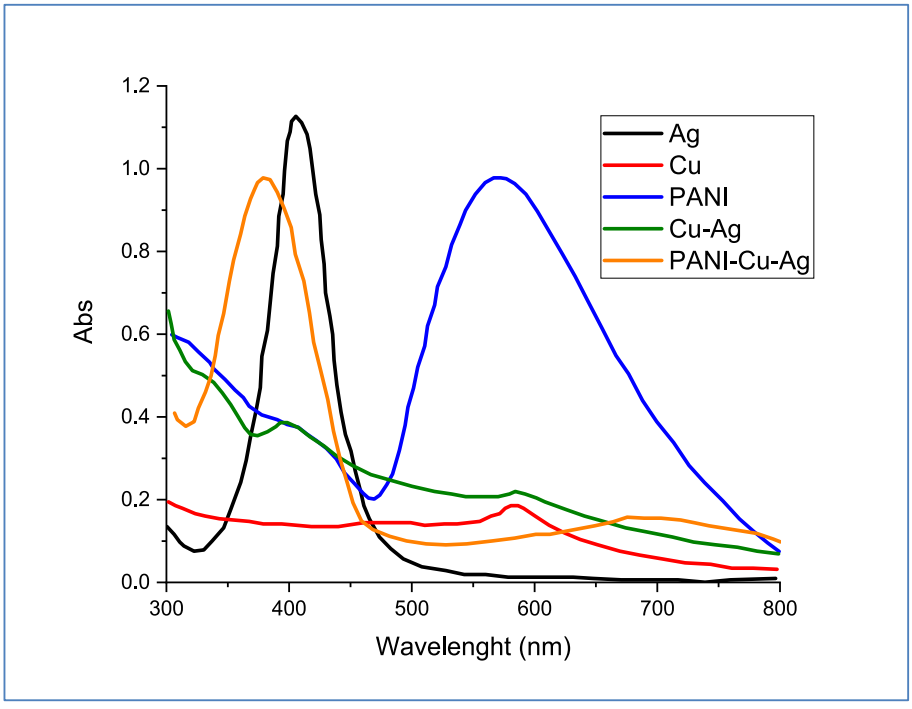

Fig. 2. UV–Vis spectrum of prepared nanocomposite.

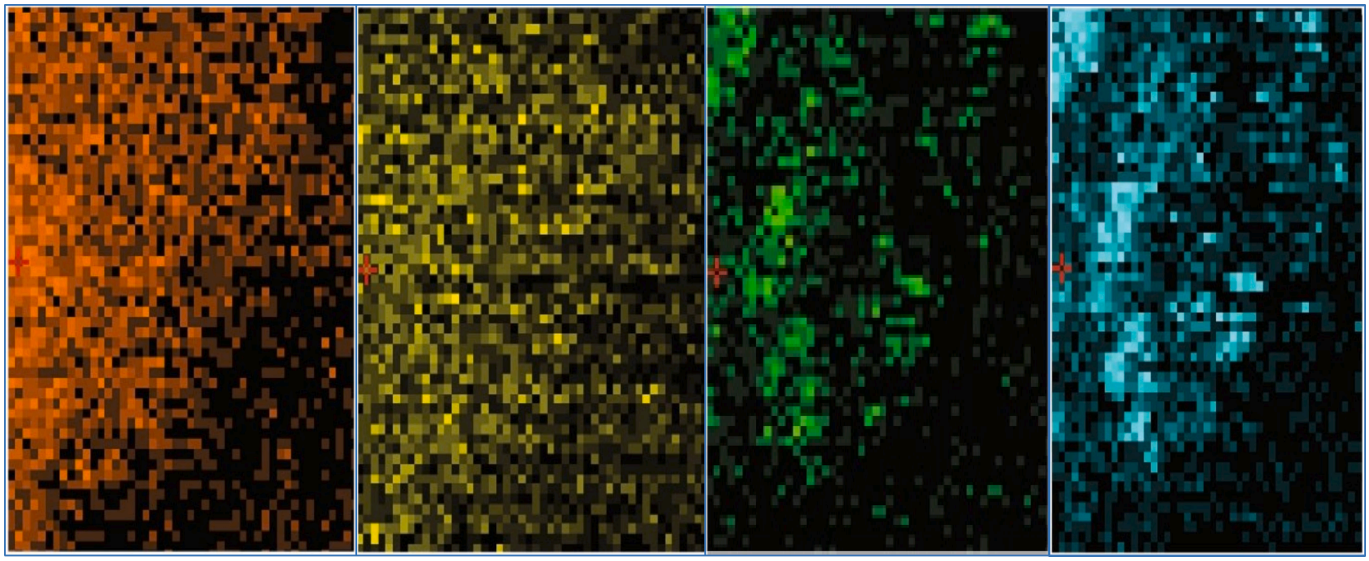

Fig. 3. Dark field-emission of Ag-Cu bimetallic nanoparticles.

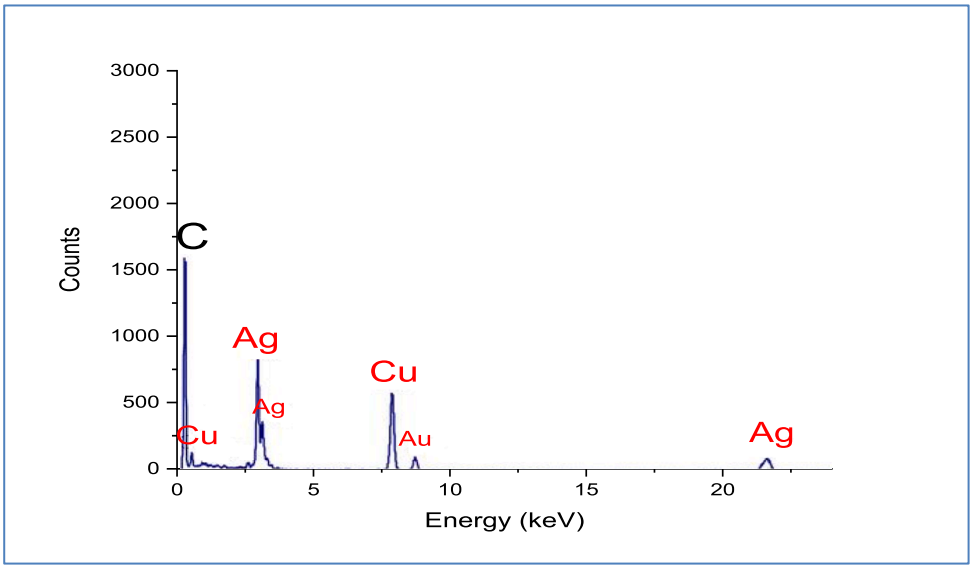

Fig. 4. EDX spectrum of Ag-Cu nanoparticles.

make strides treatment results, in this way requiring the improvement of particular techniques for overseeing and checking dopamine levels. Subsequently, exact and solid location of dopamine and hydroquinone is vital for clinical determination and natural assurance.

Until presently, an assortment of characterization and expository strategies, counting HPLC [6], GC [7], and fluorescence [8], have been created for the measurement of dopamine and hydroquinone. Electrochemical strategies are known for their quick reaction, effortlessness, favorable results, and cost-effectiveness, making them well-suited for reasonable and versatile applications [9,54–57]. Current reports do not provide evidence of synchronous electrochemical location for dopamine and hydroquinone. Hence, it is fundamental to carefully consider the improvement and determination of reasonable cathode modifiers for their electroanalytical assurance. The bimetallic framework is anticipated to show not as it were the combined characteristics of two metals, but moreover modern properties coming about from the synergistic interaction between distinctive metals [10,58–61]. The agreeable impact of bimetallic compounds can illustrate expanded action in comparison to monometallic compounds, indeed at low concentrations. Different bimetallic compounds, such as Au-Pt [11], Au-Ag [12], and Pd/Au [13], have been recognized as heterogeneous catalysts. It has been recommended that the action of bimetallic compounds is on a very basic level connected to their scattering and measure. Bimetallic compounds with a contract run of molecule sizes and great scattering are considered best for accomplishing tall action due to their lifted surface-to-volume proportion [14]. Be that as it may, nanoparticles tend to total when subjected to electrolytic applications due to their tall surface vitality, possibly restricting their viability [15,16]. As a result, elective compounds like CNTs and polymers are utilized to back and stabilize these compelling nanoparticles [17,61–65].

Polymer-based materials, such as polyaniline nanotubes (PANI nanotubes), possess inherent carrier mobility, exceptional surface area, and environmental stability, making them crucial for withstanding external electric field interference during the electric field disclosure process [18–20]. PANI nanotube sensors exhibit strong response and exceptional selectivity [21,36–40]. Conversely, bimetallic nanocomposites have been widely studied among metallic nanoparticles [21,64–69]. Guo et al. employed the ion exchange method in the

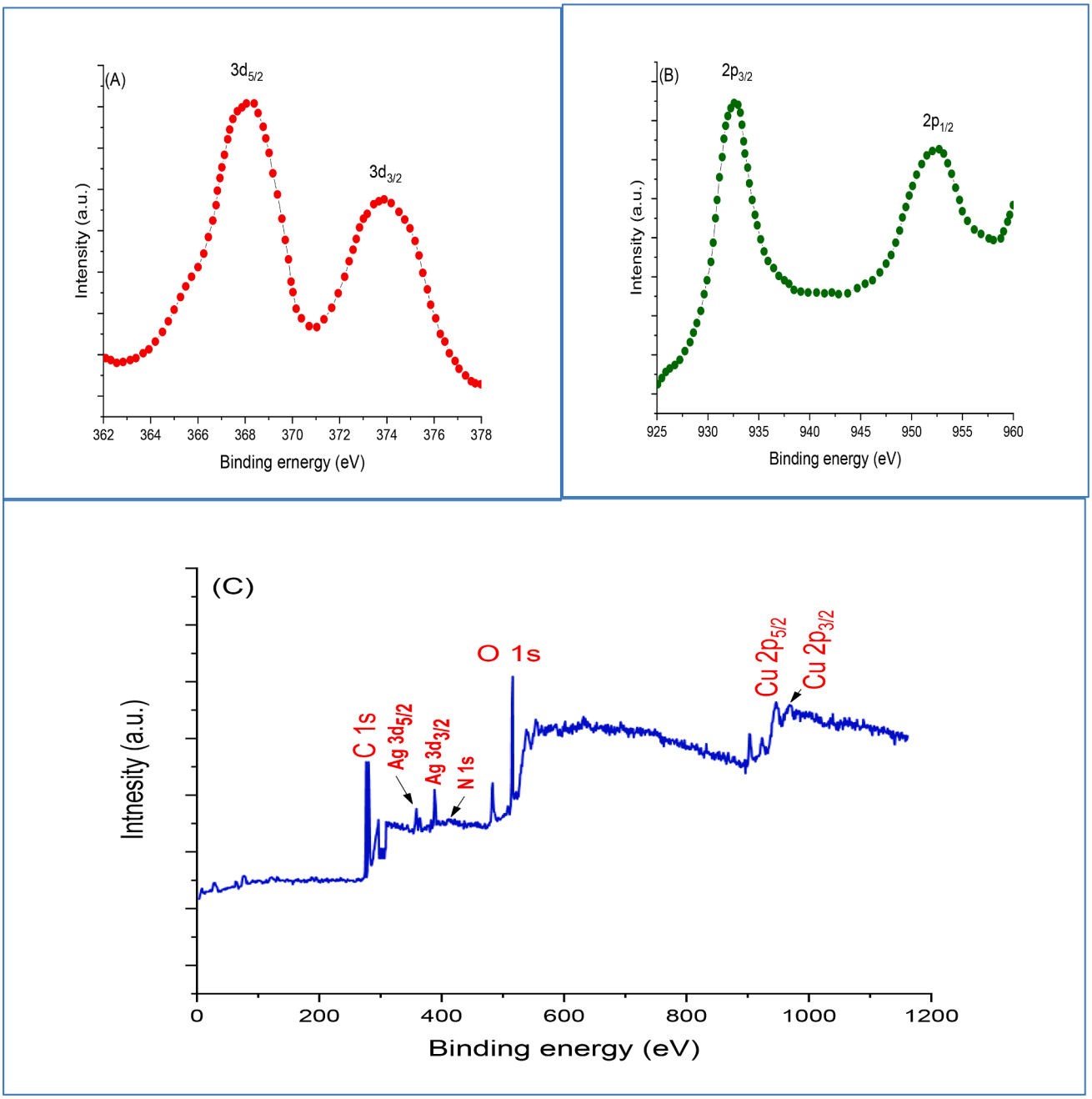

Fig. 5. XPS spectrum of PANI/Cu-Ag (a) Ag, (b) Cu and (c) survey spectrum.

preparation of well-structured (Co-Ni) OH for energy-related applications [22,41–43], while Song et al. developed Co-Ni-based carbonates by optimizing the Co/Ni atomic ratio, demonstrating excellent rate performance in asymmetrical solid-state supercapacitors [23,49]. Liao et al. reported using rGO/Ni@Co in electrochemical sensor application for determining of dopamine [24]. These studies showed the bimetallic composites potential could be used in electrochemical sensing. The research involved the synthesis of bimetallic Ag-Cu@PANI nanocomposites using co-precipitation and hydrothermal methods, followed by electrochemical testing. The Ag-Cu@PANI nanocomposite is expected to exhibit enhanced sensitivity for the simultaneous detection of dopamine and hydroquinone. Polyaniline and its derivatives modified with bimetallic have already been employed in biosensor and electrochemical applications because of their sensing features and the possibility of tuning their structure via a suitable choice of materials. Since PANI enjoys from two couples of redox, there is no requirement for any mediator in biosensor application, such that it is a self-contained mediator. In the present work the nanosensor (PANI/Cu-Ag) was synthesized and examined for selectivity and sensitivity towards dopamine and hydroquinone, and its performance was compared to different reported electrodes.

2. Materials and method

2.1. Chemical materials

All chemical materials were supplied from Merck Co., analytical grade and utilized without future purification. Aniline (98 %), hydrochloric acid (35 %), ammonium persulphate (97 %), ethanol (70 %), copper nitrate were supplied from Merck & Co.,. Sliver nitrate (99 %), hydrazine (98 %) and phosphate buffer solution (97 %) were purchased from Sigma-Aldrich.

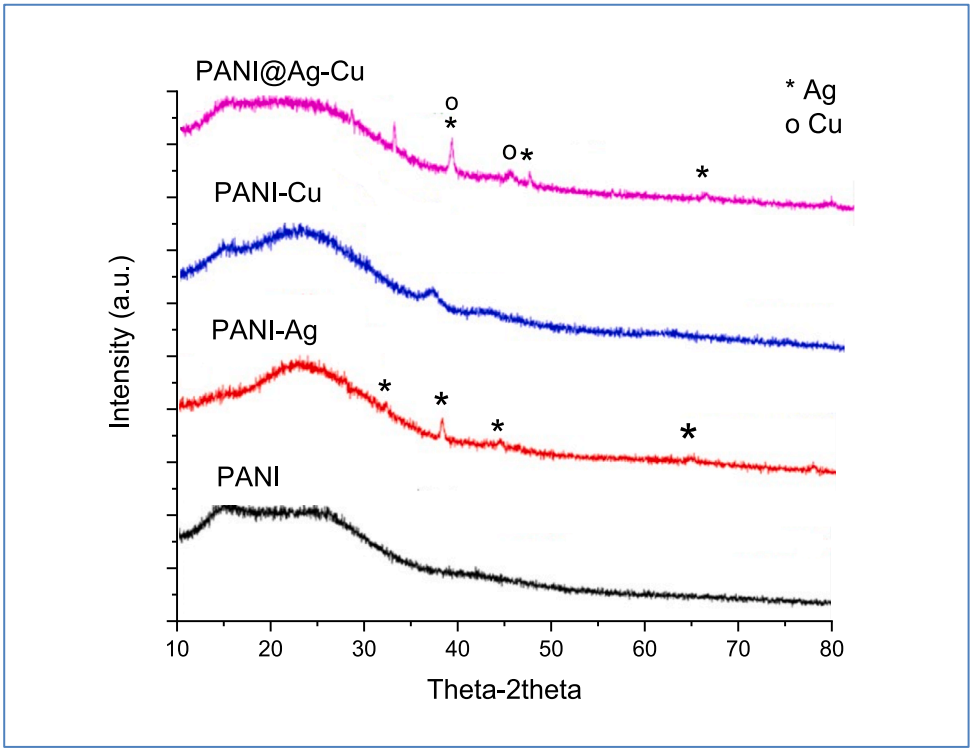

Fig. 6. XRD spectrum of PANI, and Ag, Cu and Ag-Cu@PANI nanocomposite.

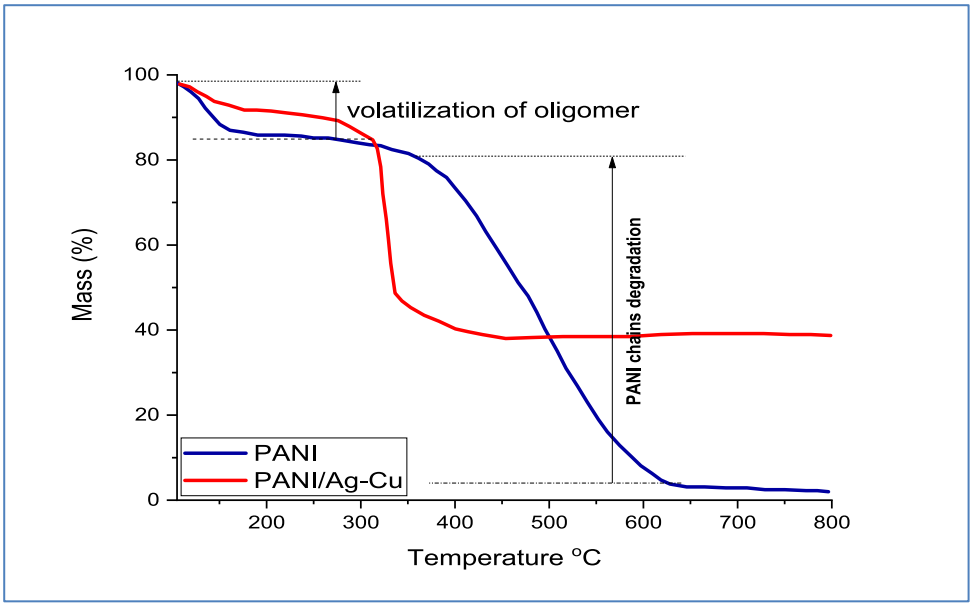

Fig. 7. TGA of PANI and PANI/Cu-Ag nanocomposite.

2.2. Synthesis of polyaniline nanotube (PANI nanotube)

Briefly, 0.5 g, 0.2 g, and 10 ml of copper nitrate, silver nitrate and hydrazine were added to the pretreated PANI and 100 ml distilled water in a 200 ml round bottom flask. Then, the mixture was refluxed for 3 h at 80 °C. The formed precipitate was isolated and washed with acetone and distilled water, followed by drying at 70 °C for 5 h. Full procedure is shown in Fig. 1.

2.3. Synthesis of Ag-Cu@PANI tubes

Briefly, 0.5 g of PANI was dispersed in 50 ml absolute ethanol ultrasonically for 30 min. After that, 0.5 g, 0.2 g, 10 ml of copper nitrate, silver nitrate and hydrazine were added to pretreated PANI and 100 ml distilled water in a 200 ml round. Then, the mixture was refluxed for 3 h at 80 °C. The formed precipitate was isolated and washed by acetone and distilled water, followed via drying at 70 °C for 5 h. Full procedure is shown in Fig. 1.

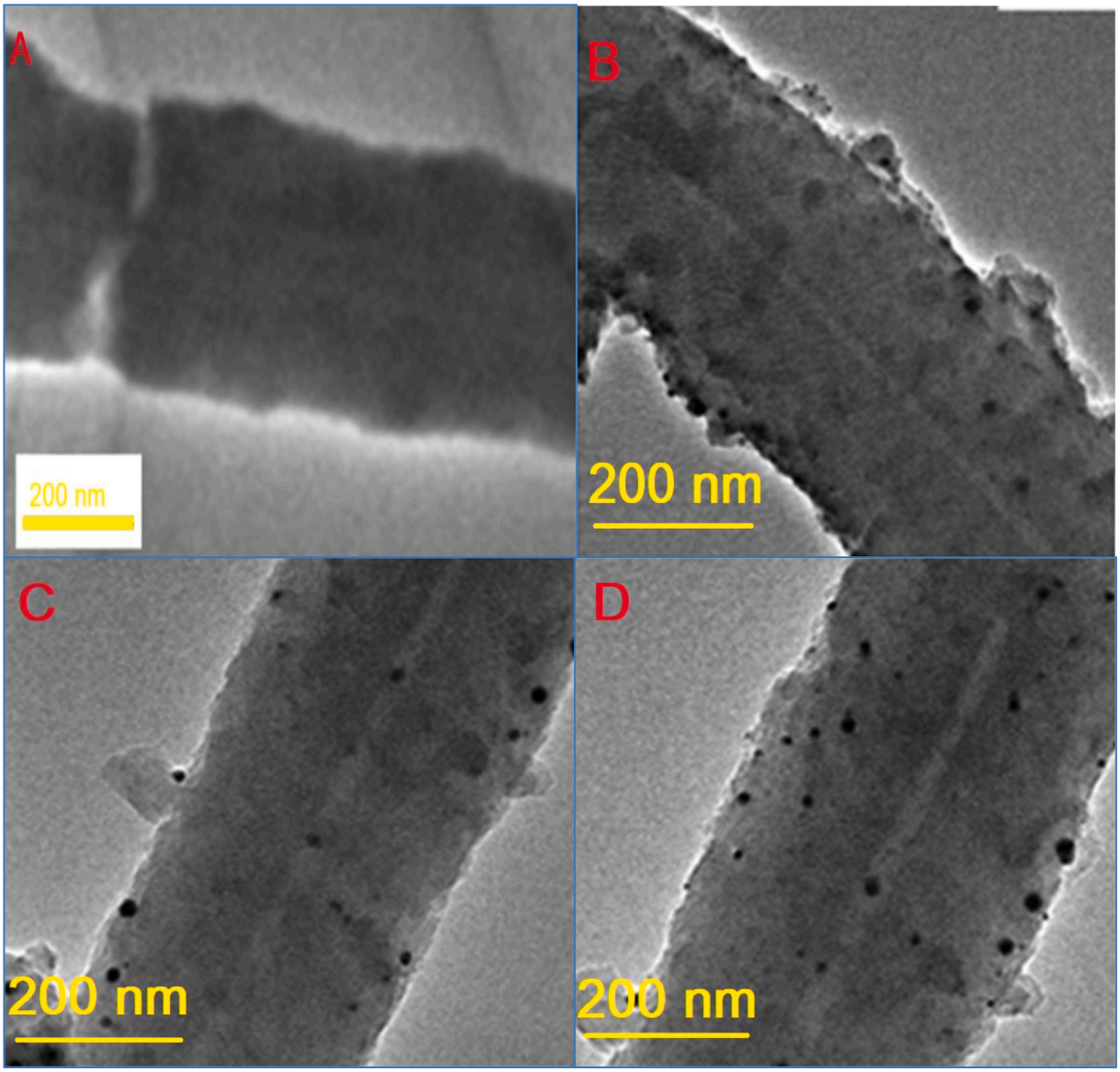

Fig. 8. TEM of (A) PANI, (B) PANI-Ag, (C) PANI-Cu, (D) PANI@Ag-Cu nanocomposite.

2.4 Electrochemical measurement

In this consider, a Normal three-electrode setup comprising of an Ag/AgCl (immersed KCl) reference anode, a platinum wire counter cathode, and an altered smooth carbon working anode was utilized, with a 0.1 M phosphate buffer arrangement at pH 7 serving as the electrolyte. The glassy carbon working electrode was cleaned by deionized water and polished it by alumina slurry. Electrochemical estimations were conducted utilizing cyclic voltammetry over the run of −0.2 to 1.2 V at a check rate of 50 mV/s, and differential beat voltammetry with a voltage step of 5 mV. Earlier to experimentation, the electrochemical cell was cleansed with N_2 gas to dispense with O_2, empowering the era of standard bends based on unmistakable flag reactions for changing concentrations of dopamine and hydroquinone.

3. Results and discussion

3.1. Bimetallic nanoparticle characterization

The UV–Vis spectrum of synthesized Ag, Cu, PANI, Ag-Cu bimetallic and PANI/Cu-Ag nanoparticles are shown in Fig. 2. The spectrum exhibited a broad adsorption band located between 380 to 580 nm with maximum adsorption peak at 425 nm related to Ag nanoparticles. The Cu metal show (red spectrum) a broad absorption band with a weak peak about 585 nm [25]. The spectrum of PANI (blue spectrum) appears two peaks at 317 and 573 back to p-p* and n-p* transitions, that assign to benzenoid and quinonoid rings structure, respectively [25]. For Ag/Cu bimetallic (green spectrum), the absorption results show a broad band at range of 300–800 nm with two weak peaks at 410 nm and 585 nm corresponding to Ag and residues of Cu and collective oscillation of Cu surface Plasmon [26]. As can be shown, a distinctive spectrum was exhibited when the Ag and Cu were measured separately. However, for Ag-Cu NPs, a spectrum matching Cu NPs was noted, proposing the production of Ag-Cu core shell NPs. Similar findings have been noted in various bimetallic NPs synthesis [27]. In comparison with PANI, the two peaks at 317 and 573 nm were shifted to 379 and 687 nm in PANI/Ag-Cu (orange spectrum). These changes are related to the presence of high intensity band formed by the reaction between the PANI chains and Ag/Cu NPs. Because of the electrostatic reaction, Ag/Cu bimetallic have a large quantity of free electrons, that facilely coordination with N atoms in PANI chains. Once PANI chains gets coordinated or imbibed with Ag/Cu, an electron cloud between PANI and Ag/Cu is formed facilely,

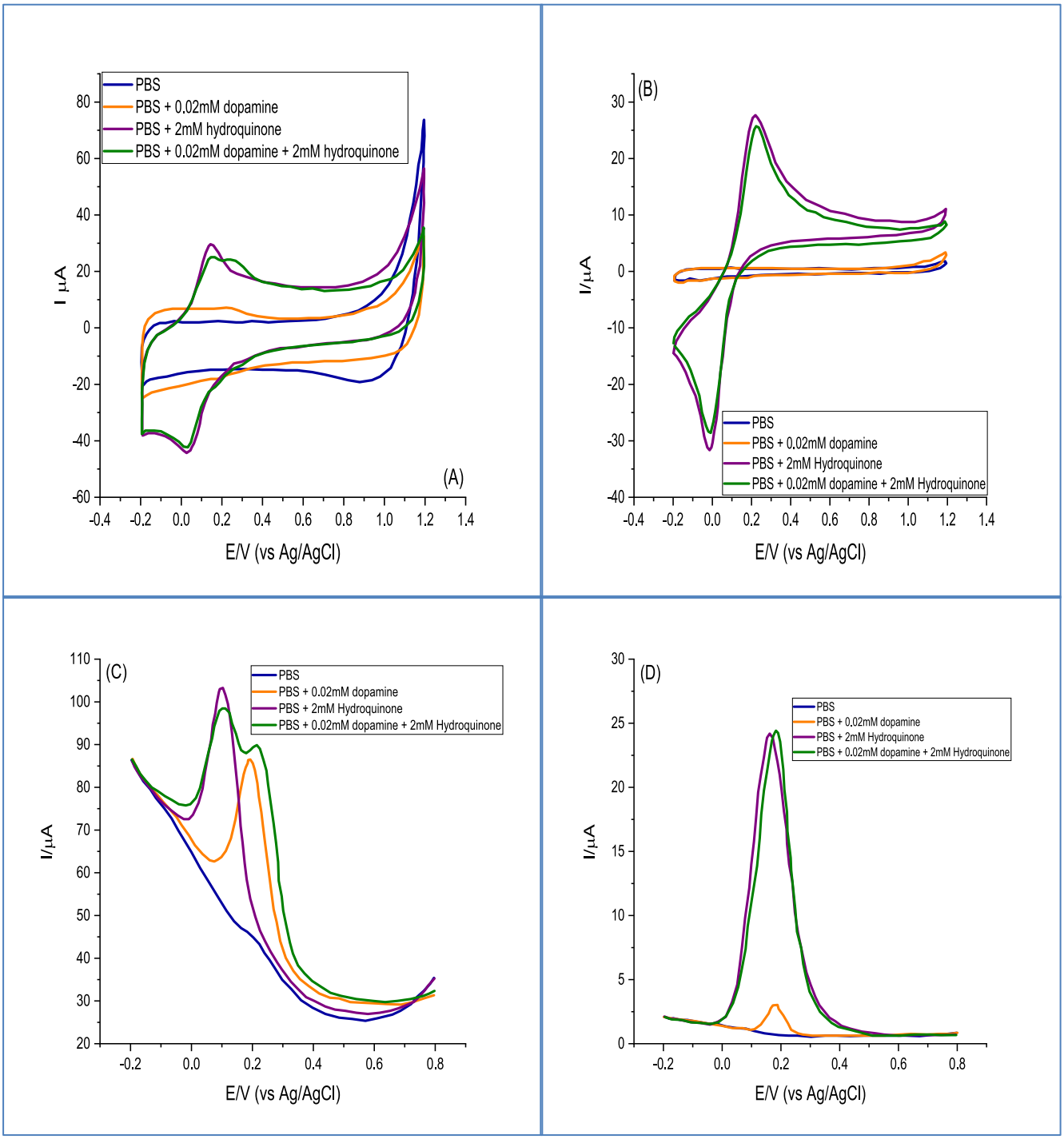

Fig. 9. CV curves of Ag-Cu@PANI (A) bare GCE, (B) in (0.01 M, pH 7) PBS at 50 mV/s scan rate, along with the DPV curves for Ag-Cu@PANI (C) bare GCE, (D) in (0.01 M, pH 7) PBS.

leading to red shift in spectra of PANI/Ag-Cu. The electron cloud formed polarons that it caused high conductivity for fabricated electrode and enhance the sensitivity [27].

Dark-field microscopy was utilized for the validation of prepared Ag-Cu bimetallic nanoparticles. The results (Fig. 3) revealed a clear coexistence of Cu and Ag within the selected field, thus facilitating the formation of Ag-Cu bimetallic nanoparticles. Furthermore, additional examination involving energy-dispersive X-ray spectroscopy (EDX) was conducted to demonstrate an elemental spectrum in the synthesized sample. Fig. 4 exhibits the EDX spectra of prepared Ag-Cu NPS. The results show the binding energy at 3, 3.1, 21.4 keV and 0.51, 7.8 keV corresponding to Ag and Cu. The elemental composition of the bimetallic NPs was determined using energy-dispersive X-ray spectroscopy (EDX), revealing that the Ag/Cu composition consisted of 59 % silver and 41 % copper.

XPS technique was used to determine the oxidation state and composition of Ag/Cu bimetallic nanoparticles. As shown in Fig. 5a, two peaks located at 368.09 and 373.04 eV back to the 3d5/2 and 3d3/2 Ag (0) electronic state, respectively. The binding energy difference between two splitting confirms the zero-oxidation state of silver in bimetallic [27]. As displayed in Fig. 5b, two binding energy related to Cu located at 932.4 and 952.6 eV was also noted, which corresponding to 2p3/2 and

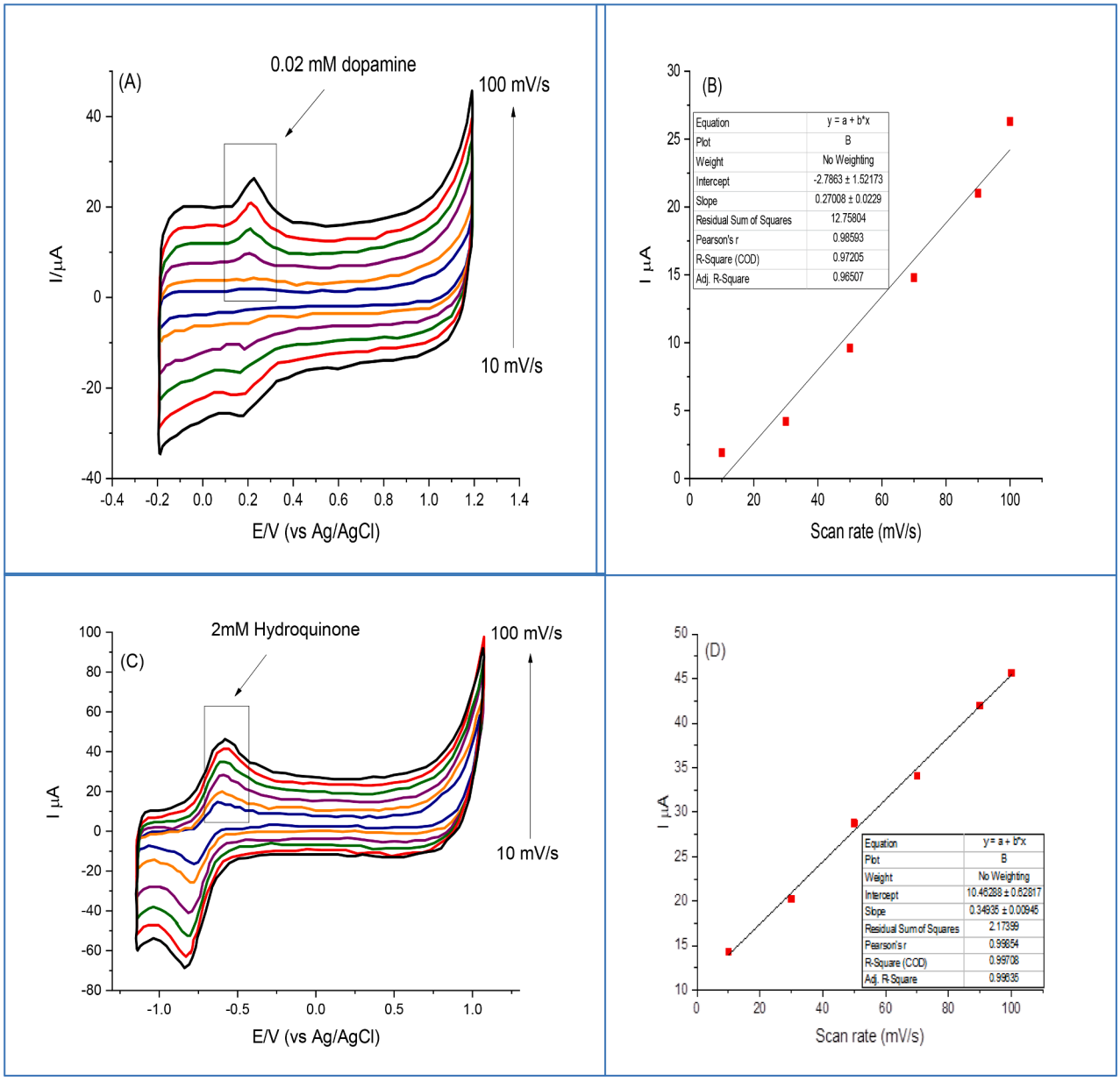

Fig. 10. CV of (A, C) dopamine and hydroquinone on Ag-Cu@PANI in 0.1 M PBS, (B,D) correlation relationship between redox peak and scan rate for dopamine and hydroquinone.

2p1/2 zero electronic state of copper [27]. The existence of other binding energy peaks (Fig. 5C, survey spectrum) at 285.03, 531.04, 400.34 could be related to C 1s, O1s and N 1s of polyaniline.

The X-ray diffraction (XRD) technique was used to study the crystalline characteristics of PANI nanotubes prepared with pure silver (Ag), copper (Cu), and Ag-Cu incorporation. The findings are presented in Fig. 6. For PANI nanotubes (Black spectrum), the XRD pattern show only wide diffraction peak centered at 2θ (17.1o), indicating PANI nanotubes. However, PANI nanotube incorporated Ag nanoparticles XRD spectrum (Red spectrum) shows four diffraction peaks located at 38.5, 44.7, 64.8 and 77.8o, corresponding to Ag face centered cubic FCC (JCPDF no. 04-0783). Fig. 6 (purple spectrum) illustrates the X-ray diffraction (XRD) spectrum of Ag-Cu@PANI nanotubes, indicating no significant shifts in peaks. This suggests that the Ag-Cu nanoparticles maintain the same phase, and also implies that their crystal structure remains unchanged during the polymerization process with PANI [28].

The thermogravimetric analysis (TGA) was used to investigated the thermal properties of PANI, and PANI/Cu-Ag. The results appear (Fig. 7) that the reduce in mass under 100 °C assign to the humidity removal [28]. At range of 100–300 °C, the loss of mass is small, which is at most because of the volatilization of oligomer dopants with low molecular weight of Cl that used through polymerization of aniline and it change in molecular weight of PANI and increase in crystallinity. At 400 °C, the PANI chains starts to thermally degrade to produce a large quantity of weight loss, leading to interior structure breakdown, large quantities of dopants and degradation of chains [28]. After that, from 600-800 °C, it become to be stable and the loss of mass is considerably decreased. The PANI/Cu-Ag exhibits a comparable degradation temperature of polyaniline at 250.5 °C, but less mass loss at 400 °C, indicating an improvement in the thermal stability of PANI due to the presence of Cu metal in PANI. The adding Ag-Cu to PANI worked to enhance the thermal stability because of interaction Ag-Cu bimetallic nanoparticles with NH_2/N═N groups in PANI chains and this caused inhibits PANI chains transfer, which is useful to enhance the thermal features of PANI/Ag-Cu nanocomposite.

The PANI nanotubes appear as short rods with a diameter of

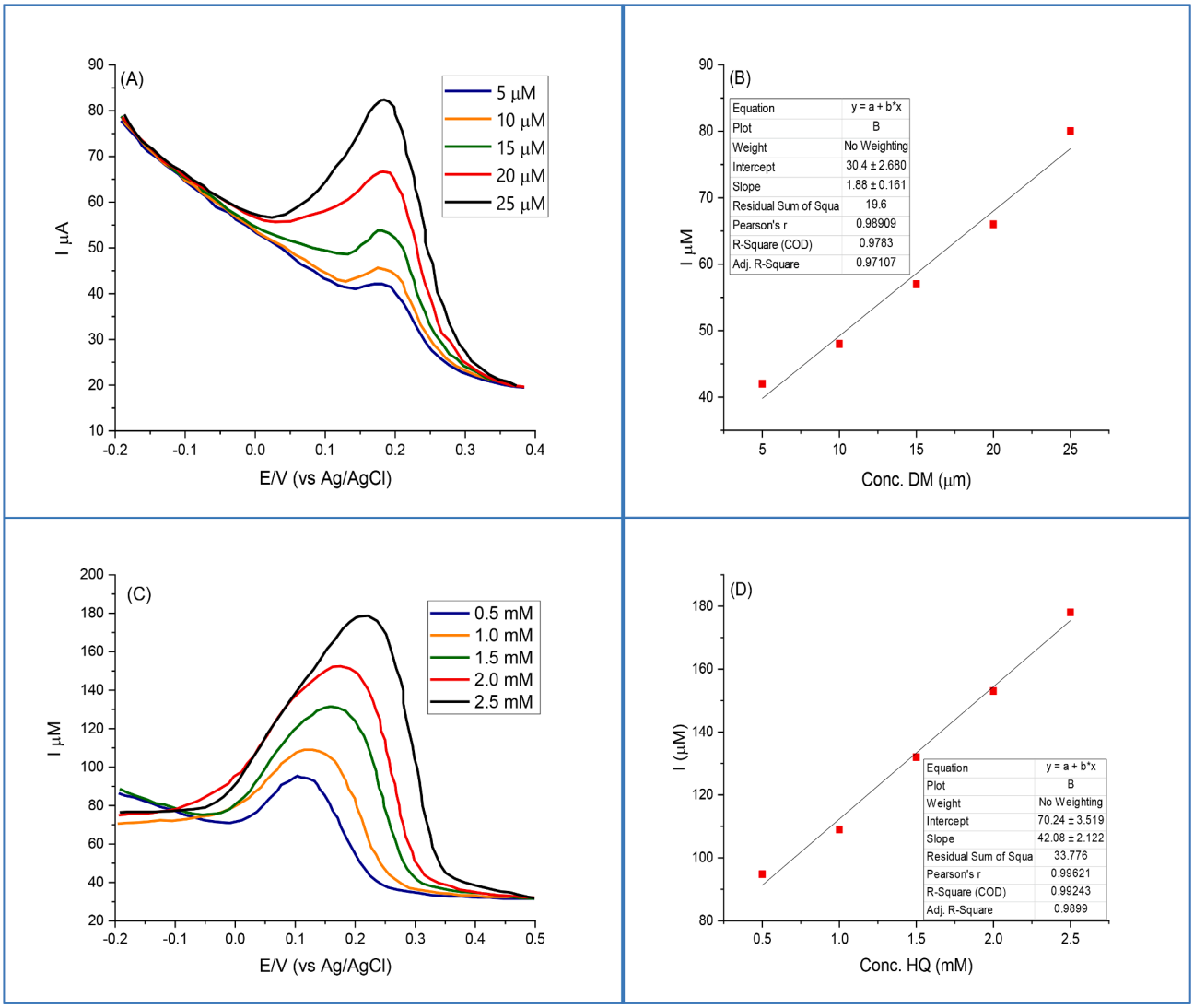

Fig. 11. DVP response of (A,C) dopamine and hydroquinone on Ag-Cu@PANI electrode with (B,D) current relationship.

300–400 nm, exhibiting a noticeable degree of twisting possibly attributed to the presence of NH groups on their surface. Analysis of TEM images reveals that the PANI nanotubes are hollow, forming a tubular structure with an internal diameter of 350–400 nm. Clearly, it's important to note that the end of PANI nanotube are closed, which may be back to high energy used through the ultrasonic irradiation reaction. After that, the PANI nanotube was used as support to the Ag-Cu NPs by using hydrazine. Then, hydrazine was used as the reducing agent and the synthesized PANI nanotubes were used as supports for Ag-Cu NPs. The PANI nanotubes containing Ag-Cu bimetallic were examined using TEM, and the findings are depicted in Fig. 8a–d. The results indicated that the diameter of the Cu-Ag NPs falls within the range of 10–20 nm. Furthermore, it was observed that Ag-Cu was uniformly distributed on the outer wall of the PANI nanotubes, maintaining the original morphology of PANI without aggregation during hydrazine co-reduction. This suggests that the prepared nanotubes possess abundant OH groups, providing numerous sites for coordination with Ag-Cu bimetallic nanoparticles [29].

3.2. Electrochemical characterization

The electrochemical behavior of dopamine and hydroquinone were explored utilizing cyclic voltammetry (CV) and Differential pulse voltammetry (DPV), as shown in Fig. 9. Both dopamine and hydroquinone displayed distinct redox peaks on the Ag-Cu@PANI electrode, showing significantly enhanced peak currents compared to GCE, as illustrated in Fig. 9A and B. In contrast, dopamine did not exhibit distinct peaks on the bare GCE, while hydroquinone displayed a broad peak in CV measurements. Fig. 9A shows that the electrochemical reaction of dopamine and hydroquinone on the Ag-Cu@PANI is considerably improved, with a higher current of oxidation peak compared with GCE. The dopamine oxidation peak is observed at 196 mV, and a distinct oxidation peak at 100 mV is indicative of the improved reversibility of hydroquinone on the Ag-Cu@PANI. These findings suggest that the electron transport on the Ag-Cu@PANI electrode is more efficient compared to the bare GCE, indicating that Ag-Cu can facilitate electron transfer. Furthermore, the 96 mV differentiation in oxidation between dopamine and hydroquinone could indicate the promising selectivity and reversibility of the Ag-Cu@PANI electrode for analyzing these compounds [30–32]. The DPV response (Fig. 9C and D) revealed overlapping reduction peaks for dopamine and hydroquinone, challenging their distinctiveness. This observed electrochemical behavior is attributed to the superior conductivity and extensive electrochemically active surface area of the Ag-Cu@PANI electrode.

Examining the kinetics of the electrode provides valuable insights into the influence of scan rate on the Ag-Cu@PANI modified electrode. The comprehensive cyclic voltammetry (CV) analysis in a 0.01 M phosphate buffer solution reveals that the currents associated with the

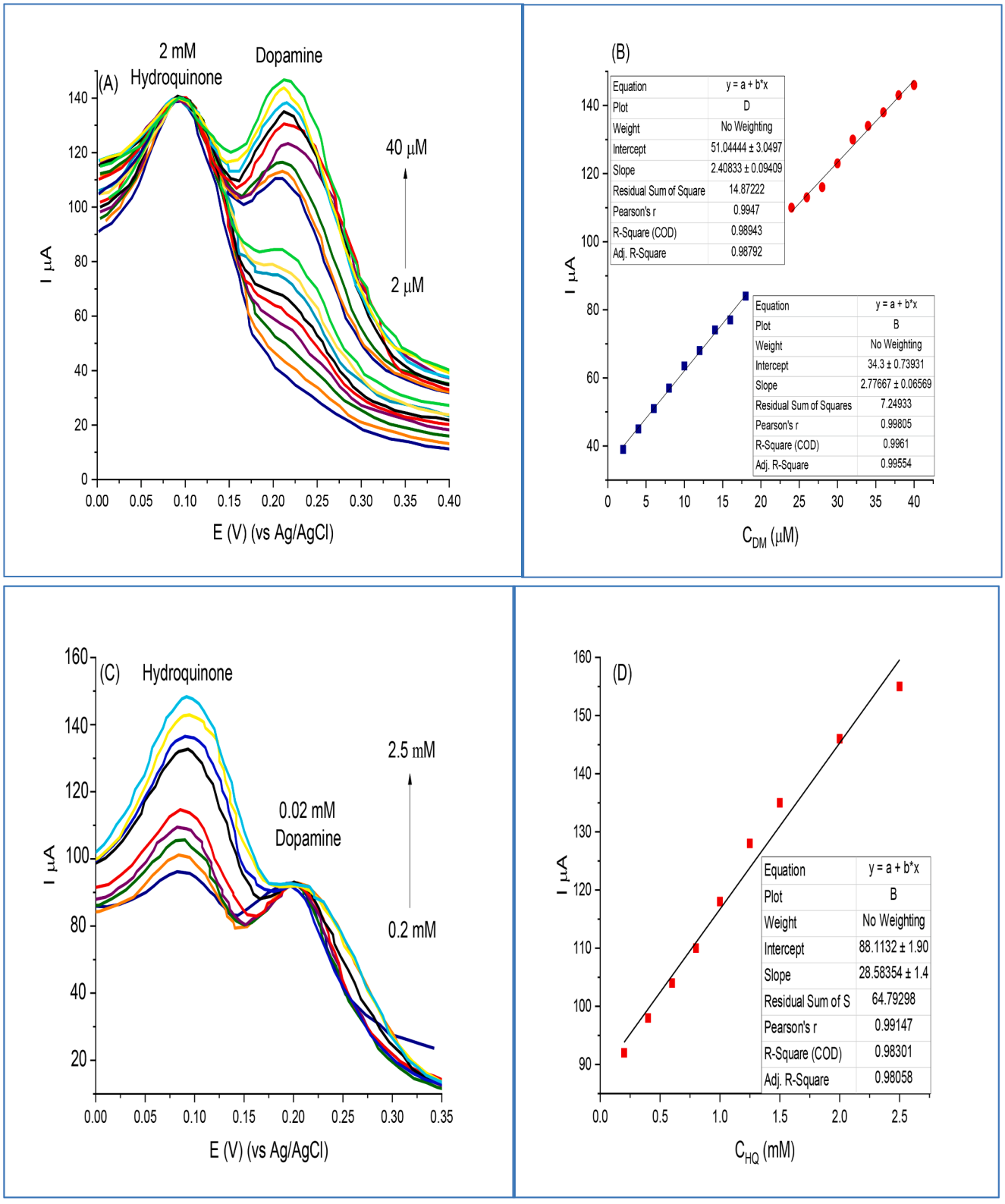

Fig. 12. DVP curve of Ag-Cu@PANI electrode for (A,C) 20–40 μM of DA and 0.2–2.5 μM of HQ and (B,D) linear oxidation peak current-DA and HQ relationship.

peak redox reactions of dopamine and hydroquinone exhibit an increase when the scan rates are expanded within the range of 10–100 mV/s, as depicted in Fig. 10A and C. The results exhibited (Fig. 10B and D) a linear relationship depicted via the two equation ip = 2.76 + 0.27*v (R^2 = 0.97) and *ip* = 10.64 + 0.34*v (R^2 = 0.99) assigned to dopamine and hydroquinone respectively. The findings suggest that the electrochemical interplay between dopamine and hydroquinone on the Ag-Cu@PANI modified surface is linked to the adsorption-controlled model, and these results align with previous research [33].

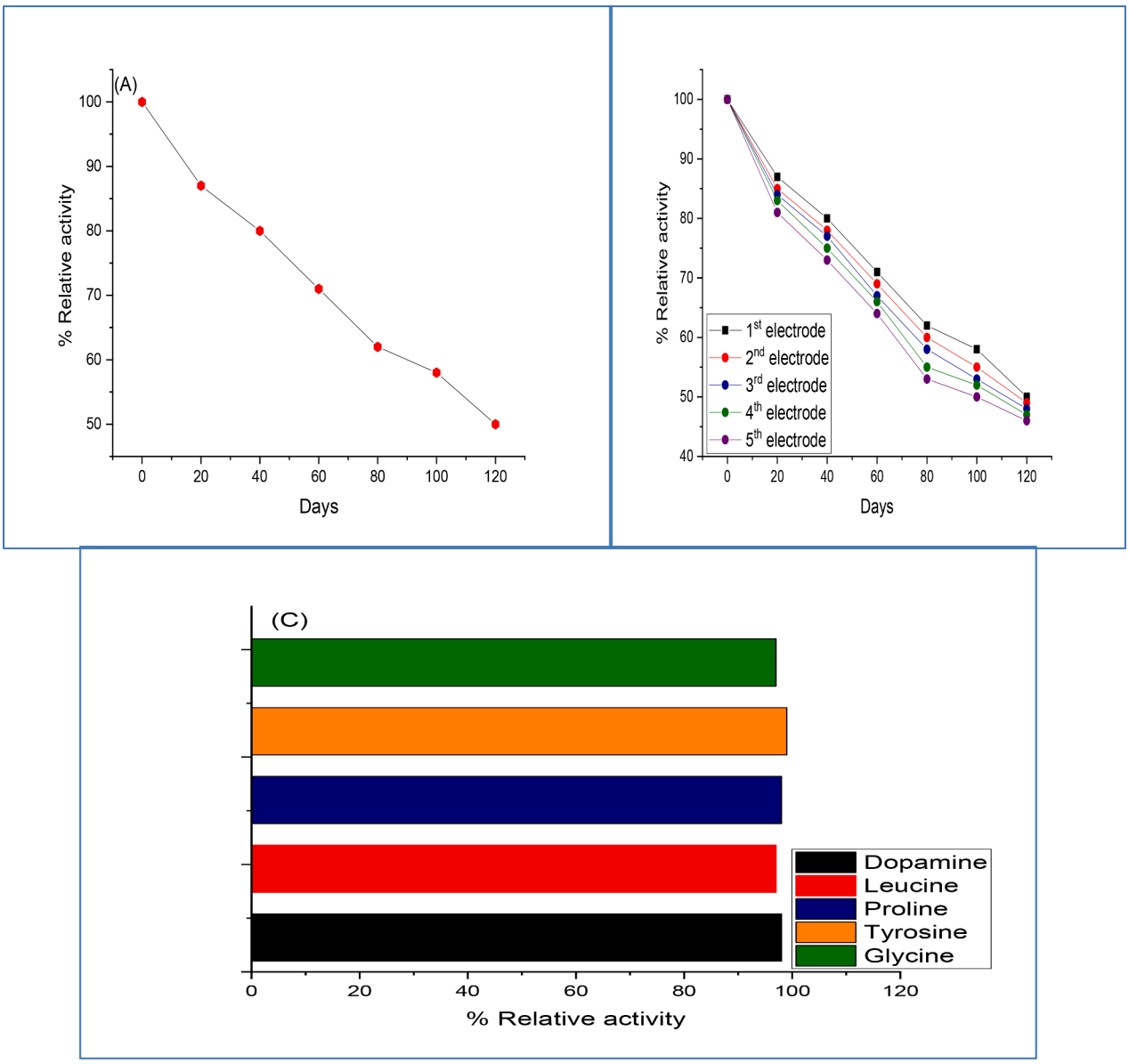

Fig. 13. (A) Biosensor response under 5 °C storage condition, (B) Storage stability impact on five similar fabricated biosensor (C) the relative activity of fabricated sensor in different amino acid.

Table 1
Electrochemical detection of dopamine with different biosensor.

No.	Electrode	LoD	Linear range	Method	Reference
1	rGO/Mn-TPP/ GCE	8 nM	0.3–188.8 μA	Amperometry	[45]
2	Porphyrin-rGO/ GCE	0.009 μM	1–70 μM	DPV	[46]
3	MWCT/Ag	0.27 μM	0–8 μM	DPV	[47]
4	CuTPP/rGO/ GCE	0.58 μM	2–200 μM	CV, DPV	[48]
5	PANI/Cu-Ag	0.46 μM	5–25 μM	CV, DPV	Our study

Table 2
Electrochemical detection of hydroquinone with different biosensor.

Modified electrode	Analyte	Linear range (mM)	Method	Reference
AuNPs-CNF/Au	hydroquinone	9–500	DPV	[50]
Au/pAMT-MWNTs	hydroquinone	7.2–391.2	CV	[51]
AuNPs/Fe_3O_4-APTESGO/GCE	hydroquinone	3–137	DPV, CV	[52]
PDA-RGO/GCE	hydroquinone	1–230	DPV, CV	[53]
PANI/Cu-Ag	hydroquinone	0.5–25	CV, DPV	Our study

3.2.1. Electrodetermination of dopamine and hydroquinone on the Ag-Cu@PANI electrode

DPV measurements provides more sensitivity and selectivity compared to CV measurements as displayed in Fig. 11A and C. By utilizing DPV, we measured and estimated a broad range of dopamine and hydroquinone concentration from (5–25 μM) and (0.5–2.5 mM) respectively, in incrementally boosting batches. As shown in Fig. 11B and D, a linear relationship was noted between the current of oxidation peak and concentration of dopamine and hydroquinone, obtained via two following equations i (10^{-6}A) = 1.88 + 30.4*c (R^2 = 0.98) and i (10^{-6} A) = 42.08 + 70.24 *c (R^2 = 0.99) [34,35].

3.2.2. Simultaneous determination of dopamine and hydroquinone using Ag-Cu@PANI electrode

The calibration curves and limit of detection for Ag-Cu@PANI electrode in dopamine and hydroquinone simultaneous sensing were initiated by using DPV measurements in 0.1 M PBS. At a consistent hydroquinone concentration of 0.002 M, the response of differential pulse voltammetry (DPV) to dopamine displayed a linear correlation within the 2–40 μm range. The results (Fig. 12B) show linear equations as described $i\ (10^{-6}A) = 2.77 + 34.3x$ ($R^2 = 0.99$) and $i = 2.40 + 51.04x$ ($R^2 = 0.98$). Furthermore, as depicted in Fig. 12c, at a consistent dopamine concentration of $1*10^{-5}$ M, the differential pulse voltammetry (DPV) response to hydroquinone demonstrated a direct correlation within the same concentration range of 0.2–2.5 μM, as indicated by the following equation $i\ (10^{-6}\ A) = 28.69 + 88.11x$ ($R^2 = 0.98$) (0.002 M) (Fig. 12D). The findings suggest that the Ag-Cu@PANI modified electrode may be effectively utilized for the concurrent detection of dopamine and hydroquinone, yielding positive outcomes.

3.2.3. Stability and reproducibility of the suggested electrochemical sensor

To assess the reproducibility of the Ag-Cu@PANI electrode, five electrodes were fabricated using a consistent method and tested for their oxidation peak current values for dopamine and hydroquinone. The observed currents exhibited minimal variations, with relative standard deviations (RSD) of 1.54 % for dopamine and 2.45 % for hydroquinone, indicating favorable reproducibility. Additionally, cyclic voltammetry (CV) measurements were conducted over 20 cycles in a 0.2 M PBS solution containing 20 μM dopamine and 0.002 M hydroquinone. It is noteworthy that the redox peak currents for dopamine and hydroquinone remained stable throughout the measurements, with the final cycle retaining over 98 % of the initial peak current value, confirming the precision of the Ag-Cu@PANI sensor. On the other side, to evaluate the stability of the fabricated PANI/Cu-Ag electrode with time, the current response was estimated via storing it at 5 °C. The results (Fig. 13A) display that the fabricated electrode kept 50 % of the primary activity after employing it 100 times for 120 days, demonstrating significant agreement with earlier reported [44]. Five dopamine and hydroquinone electrodes were fabricated and investigated separately for the impact of storage at 5 °C. The results (Fig. 13B) appeared high stability for fabricated sensor, which indicate to a reproducible performance. To observe the interference impact of different compounds on the sensing capability of PANI/Ag-Cu to dopamine, different amino acid such as leucine, proline, tyrosine and glycine were added at pH 7 buffer. The results shown no observable interference concerning the increasing or reduce in relative activity for the dopamine (Fig. 13C). Hence, its concluded that the fabricated sensor can selectivity reveal or detect in biological samples.

Table 1 displays some reported dopamine sensor-based nanocomposite and their comparison with our fabricated sensor in linear range, LoD and sensitivity. The results show that displayed better execution and nearly comparable performance with relate to range of concentration, LoD and sensitivity.

Table 2 displays some reported hydroquinone sensor-based nanocomposite and their comparison with our fabricated sensor in linear range. The results show that displayed better execution and nearly comparable performance with relate to range of concentration sensitivity.

4. Conclusions

In this study, we can list the main point as following:

1- bimetallic Ag-Cu doped PANI nanotubes composite (Ag-Cu@PANI) was successfully prepared by reduction method.
2- The electrochemical analysis demonstrated that the Ag-Cu@PANI electrode exhibited efficient electrooxidation of dopamine and hydroquinone, making it a potential candidate for use as an electrochemical sensor for the simultaneous detection of these substances.
3- The as-suggested electrode demonstrates low limits of estimation of dopamine and hydroqiunone, while also offering a wide linear range for these substances.
4- The proposed biosensor was enhanced to concurrently detect dopamine and hydroquinone, demonstrating low detection limits of 0.46 μM for dopamine and 0.23 mM for hydroquinone, respectively.
5- Moreover, the fabricated sensor shows broad linear ranges for dopamine (5–25 μM), and hydroquinone (0.5–2.5 mM).

Data availability

All data generated or analyzed during this study are included this published article.

Funding

Not applicable.

Authors contributions

All authors' participated design the study, performed the experiments, analyzed the results, and wrote the manuscript. All authors read and approved the final manuscript.

CRediT authorship contribution statement

Mohamed J. Saadh: Formal analysis, Investigation, Writing – original draft, Writing – review & editing. **H.N.K. AL-Salman:** Formal analysis, Investigation, Writing – original draft, Writing – review & editing. **Hussein H. Hussein:** Formal analysis, Investigation, Writing – original draft, Writing – review & editing. **Zaid H. Mahmoud:** Writing – review & editing, Writing – original draft, Investigation, Formal analysis. **Hamza Hameed Jasim:** Formal analysis, Investigation, Writing – original draft, Writing – review & editing. **Zahraa hassan Ward:** Formal analysis, Investigation, Writing – original draft, Writing – review & editing. **Mahmood Hasen shuhata Alubiady:** Formal analysis, Investigation, Writing – original draft, Writing – review & editing. **Ahmed Muzahem Al-Ani:** Formal analysis, Investigation, Writing – original draft, Writing – review & editing. **Sally Salih Jumaa:** Formal analysis, Investigation, Writing – original draft, Writing – review & editing. **Hamidreza Sayadi:** Formal analysis, Investigation, Writing – original draft, Writing – review & editing. **Ehsan Kianfar:** Writing – review & editing, Writing – original draft, Investigation, Formal analysis.

Declaration of competing interest

The authors declare that they have no known competing financial interests or personal relationships that could have appeared to influence the work reported in this paper.

References

[1] M.O. Klein, D.S. Battagello, A.R. Cardoso, et al., Dopamine: functions, signaling, and association with neurological diseases, Cell. Mol. Neurobiol. 39 (2019) 31–59, https://doi.org/10.1007/s10571-018-0632-3.
[2] P. Shaikshavali, T. Madhusudana Reddy, T. Venu Gopal, et al., Development of carbon-based nanocomposite biosensor platform for the simultaneous detection of catechol and hydroquinone in local tap water, J. Mater. Sci. Mater. Electron. 32 (2021) 5243–5258, https://doi.org/10.1007/s10854-021-05256-3.
[3] Y. Pang, G.m. Zeng, L. Tang, et al., Laccase biosensor using magnetic multiwalled carbon nanotubes and chitosan/silica hybrid membrane modified magnetic carbon paste electrode, J. Cent. South Univ. Technol. 18 (2011) 1849–1856, https://doi.org/10.1007/s11771-011-0913-1.
[4] S.U. Singh, S. Chatterjee, S.A. Lone, et al., Advanced wearable biosensors for the detection of body fluids and exhaled breath by graphene, Microchim. Acta 189 (2022) 236, https://doi.org/10.1007/s00604-022-05317-2.

[5] H. Adam, S.C.B. Gopinath, M.K. Md Arshad, et al., An update on pathogenesis and clinical scenario for Parkinson's disease: diagnosis and treatment, Biotech 13 (2023) 142, https://doi.org/10.1007/s13205-023-03553-8.

[6] I. Baranowska, J. Płonka, Simultaneous determination of biogenic amines and methylxanthines in foodstuff—sample preparation with HPLC-DAD-FL analysis, Food Anal. Methods 8 (2015) 963–972, https://doi.org/10.1007/s12161-014-9972-x.

[7] L. Lu, Y. Zhou, T. Zheng, et al., SERS and EC dual-mode detection for dopamine based on WO3-SnO2 nanoflake arrays, Nano Res. 16 (2023) 4049–4054, https://doi.org/10.1007/s12274-022-4984-0.

[8] E. Hwang, B. Lee, Synthesis of a fluorescence sensor based on carbon quantum dots for detection of bisphenol A in aqueous solution, Korean J. Chem. Eng. 39 (2022) 1324–1332, https://doi.org/10.1007/s11814-021-0989-8.

[9] Y. Zhang, W. Liu, W. Yao, et al., An electrochemical sensor based on carbon composites derived from bisbenzimidazole biphenyl coordination polymers for dihydroxybenzene isomers detection, Microchim. Acta 191 (2024) 20, https://doi.org/10.1007/s00604-023-06099-x.

[10] J. Zhang, C. Hou, H. Huang, L. Zhang, Z. Jiang, G. Chen, Y. Jia, Q. Kuang, Z. Xie, L. Zheng, Surfactant-concentration dependent shape evolution of Au-Pd alloy nanocrystals from rhombic dodecahedron to trisoctahedron and hexoctahedron, Small 9 (2013) 538–544.

[11] W. Ye, J. Yu, Y. Zhou, D. Gao, D. Wang, C. Wang, D. Xue, Green synthesis of Pt−Au dendrimer-like nanoparticles supported on polydopamine-functionalized graphene and their high performance toward 4-nitrophenol reduction, Appl. Catal. B 181 (2016) 371–378.

[12] N. Arora, A. Mehta, A. Mishra, S. Basu, 4-Nitrophenol reduction catalysed by Au-Ag bimetallic nanoparticles supported on LDH: homogeneous vs. heterogeneous catalysis, Appl. Clay Sci. 151 (2018) 1–9.

[13] F. Jiang, R. Li, J. Cai, W. Xu, A. Cao, D. Chen, X. Zhang, C. Wang, C. Shu, Ultrasmall Pd/Au bimetallic nanocrystals embedded in hydrogen-bonded supramolecular structures: facile synthesis and catalytic activities in the reduction of 4-nitrophenol, J. Mater. Chem. A 3 (2015) 19433–19438.

[14] N.s. Ahmed, C.-Y. Hsu, Z.H. Mahmoud, H. Sayadi, E. kianfar, A graphene oxide/polyaniline nanocomposite biosensor: synthesis, characterization, and electrochemical detection of bilirubin, RSC Adv. 13 (2023) 36280–36292, https://doi.org/10.1039/D3RA06815C.

[15] I.A. AbdulKareem, Z.H. Mahmoud, A.A. Khadom, Sunlight assisted photocatalytic mineralization of organic pollutants over rGO impregnated TiO2 nanocomposite: theoretical and experimental study, Case Stud. Chem. Environ. Eng. 8, 100446, doi: 10.1016/j.cscee.2023.100446.

[16] C.Y. Hsu, Z.H. Mahmoud, S. Abdullaev, B.A. Mohammed, U.S. Altimari, M.L. Shaghnab, G.F. Smaisim, Nanocomposites based on Resole/graphene/carbon fibers: a review study, Case Stud. Chem. Environ. Eng. 8, 100535, doi: 10.1016/j.cscee.2023.100535.

[17] I. Raya, H.H. Kzar, Z.H. Mahmoud, et al., A review of gas sensors based on carbon nanomaterial, Carbon Lett. 32 (2022) 339–364, https://doi.org/10.1007/s42823-021-00276-9.

[18] J. Qiao, Y. Wu, C. Zhu, et al., High-performance carbon nanotube/polyaniline artificial yarn muscles working in biocompatible environments, Nano Res. 16 (2023) 4143–4151, https://doi.org/10.1007/s12274-022-4910-5.

[19] Z.H. Mahmoud, R.A. AL-Bayati, A.A. Khadom, Synthesis and supercapacitor performance of polyaniline-titanium dioxide-samarium oxide (PANI/TiO2-Sm2O3) nanocomposite, Chem. Pap. 76 (2022) 1401–1412, https://doi.org/10.1007/s11696-021-01948-6.

[20] Z.H. Mahmoud, R.A. Al-Bayati, A.A . Khadom, In situ polymerization of polyaniline/samarium oxide - anatase titanium dioxide (PANI/Sm2O3-TiO2) nanocomposite: structure, thermal and dielectric constant supercapacitor application study, J. Oleo Sci. 71 (2) (2022) 311–319.

[21] I.Y. Isaeva, G.Y. Ostaeva, E.A. Eliseeva, et al., The structure of nanocomposites with bimetallic Cu–Ni nanoparticles obtained by chemical reduction, Crystallogr. Rep. 67 (2022) 987–995, https://doi.org/10.1134/S1063774522060104.

[22] X. Wang, H. Song, S. Ma, M. Li, G. He, M. Xie, X. Guo, Template ion-exchange synthesis of Co-Ni composite hydroxides nanosheets for supercapacitor with unprecedented rate capability, Chem. Eng. J. 432 (2022) 134319.

[23] L. Li, S. Lu, Y. Dai, H. Li, X. Wang, Y. Zhang, Controlled synthesis of hierarchical nanostructured metal ferrite microspheres for enhanced electrocatalytic oxygen evolution reaction, ACS Appl. Nano Mater. 6 (3) (2023) 2184–2192.

[24] Q. He, X. Kang, F. Fu, M. Ren, F. Liao, The synthesis of rGO/Ni/Co composite and electrochemical determination of dopamine, J. Inorg. Organomet. Polym Mater. 30 (2020) 4269–4277.

[25] K. Anandalakshmi, J. Venugobal, V. Ramasamy, Characterization of silver nanoparticles by green synthesis method using Pedalium murex leaf extract and their antibacterial activity, Appl. Nanosci. 6 (2016) 399–408, https://doi.org/10.1007/s13204-015-0449-z.

[26] G.S. Lotey, S. Kumar, N.K. Verma, Fabrication and electrical characterization of highly ordered copper nanowires, Appl. Nanosci. 2 (2012) 7–13, https://doi.org/10.1007/s13204-011-0034-z.

[27] T. Masaharu, H. Sachie, T. Ryuichi, S. Yoshiyuki, Synthesis of bicompartmental Ag/Cu nanoparticles using a two-step polyol process, Chem. Lett. 38 (8) (2009), https://doi.org/10.1246/cl.2009.860.

[28] H. Abdullah, N.M. Naim, A. Bolhan, et al., Morphology, structural and electrical properties of Ag–Cu alloy nanoparticles embedded in PVA matrix and its performance as E. coli monitoring sensor, Arab. J. Sci. Eng. 40 (2015) 915–922, https://doi.org/10.1007/s13369-014-1557-x.

[29] N.M. Naim, H. Abdullah, A.A. Hamid, Influence of Ag and Pd contents on the properties of PANI–Ag–Pd nanocomposite thin films and its performance as electrochemical sensor for E. coli detection, Electron. Mater. Lett. 15 (2019) 70–79, https://doi.org/10.1007/s13391-018-0087-1.

[30] L. Weng, Y. Yao, B. Liu, C. Yang, Millepora sp. fossil-like nickel-cobalt microsphere and its neurotransmitter electrochemical activity, J. Alloy. Compd. 826 (2020) 154087.

[31] X. Chen, X. Wang, D. Fang, Fuller. Nanotub. Carbon Nanostruct. 28 (2020) 1048–1058.

[32] X. Zheng, Z. Wang, Q. Zhou, Q. Wang, W. He, S. Lu, Precision tuning of highly efficient Pt-based ternary alloys on nitrogen-doped multi-wall carbon nanotubes for methanol oxidation reaction, J. Energy Chem. 88 (2024) 242–251.

[33] X. Zhang, S. Yu, W. He, H. Uyama, Q. Xie, L. Zhang, F. Yang, Electrochemical sensor based on carbon-supported NiCoO2 nanoparticles for selective detection of ascorbic acid, Biosens. Bioelectron. 55 (2014) 446–451.

[34] W. Sun, H. Chu, X. Zha, S. Lu, Y. Wang, Enhanced electrochemical sensing of butylated hydroxy anisole through hollow metal-organic frameworks with gold nanoparticles and enzymes, ACS Appl. Nano Mater. 6 (16) (2023) 15183–15192.

[35] Z. Liu, D. Liao, J. Yu, X. Jiang, An electrochemical sensor based on oxygen-vacancy cobalt–aluminum layered double hydroxides and hydroxylated multiwalled carbon nanotubes for catechol and hydroquinone detection, Microchem. J. 175 (2022) 107216.

[36] S.A. Jasim, H.H. Kzar, R. Sivaraman, M.J. Jweeg, M. Zaidi, O.K.A. Alkadir, E. Kianfar, Engineered nanomaterials, plants, plant toxicity and biotransformation: a review, Egypt. J. Chem. 65 (12) (2022) 151–164.

[37] M.M. Kadhim, A.M. Rheima, Z.S. Abbas, H.H. Jlood, S.K. Hachim, W.R. Kadhum, Evaluation of a biosensor-based graphene oxide-DNA nanohybrid for lung cancer, RSC Adv. 13 (4) (2023) 2487–2500.

[38] M. Fattahi, C.Y. Hsu, A.O. Ali, Z.H. Mahmoud, N.P. Dang, E. Kianfar, Severe plastic deformation: nanostructured materials, metal-based and polymer-based nanocomposites: a review, Heliyon (2023), https://doi.org/10.1016/j.heliyon.2023.e22559.

[39] G.L. Ismaeel, S.A. Hussein, G. Daminova, J.M.A. Sulaiman, M.M. Hani, E. H. Kadhum, E. Kianfar, Fabrication and investigating of a nano-structured electrochemical sensor to measure the amount of atrazine pollution poison in water and wastewater, Chem. Data Collect. 51 (2024) 101135.

[40] E. Kianfar, Protein nanoparticles in drug delivery: animal protein, plant proteins and protein cages, albumin nanoparticles, J. Nanobiotechnol. 19 (1) (2021) 159.

[41] X. Huang, Y. Zhu, E. Kianfar, Nano biosensors: properties, applications and electrochemical techniques, J. Mater. Res. Technol. 12 (2021) 1649–1672.

[42] E. Kianfar, V. Cao, Polymeric membranes on base of PolyMethyl methacrylate for air separation: a review, J. Mater. Res. Technol. 10 (2021) 1437–1461.

[43] E. Kianfar, Recent advances in synthesis, properties, and applications of vanadium oxide nanotube, Microchem. J. 145 (2019) 966–978.

[44] N.s. Ahmed, C.-Y. Hsu, Z.H. Mahmoud, H. Sayadi, E. kianfar, A graphene oxide/polyaniline nanocomposite biosensor: synthesis, characterization, and electrochemical detection of bilirubin, RSC Adv. 51 (2023), https://doi.org/10.1039/D3RA06815C.

[45] S. Sakthinathan, H.F. Lee, S.-M. Chen, et al., Electrocatalytic oxidation of dopamine based on non-covalent functionalization of manganese tetraphenylporphyrin/reduced graphene oxide nanocomposite, J. Colloid Interface Sci. 468 (2016) 120–127.

[46] M. Lv, T. Mei, X. Wang, Selective and sensitive electrochem ical detection of dopamine based on water-soluble porphyrin functionalized graphene nanocomposites, RSC Adv. 4 (2014) 9261–9270.

[47] I. Anshori, L. Nuraviana Rizalputri, R. Rona Althof, et al., Functionalized multi-walled carbon nanotube/silver nanoparticle (f-MWCNT/AgNP) nanocomposites as non-enzymatic electro chemical biosensors for dopamine detection, Nanocomposites. 7 (2021) 97–108.

[48] C. Karuppiah, S. Sakthinathan, S.M. Chen, et al., A non-covalent functionalcally reduced graphene oxide nanocomposite for the selective determination of dopamine, Appl. Organomet. Chem. 30 (2016) 40–46.

[49] J.M. Pingarrón, J. Labuda, J. Barek, C.M. Brett, M.F. Camoes, M. Fojta, D. B. Hibbert, Terminology of electrochemical methods of analysis (IUPAC Recommendations 2019), Pure Appl. Chem. 92 (4) (2020) 641–694.

[50] Z. Huo, Y. Zhou, Q. Liu, X. He, Y. Liang, M. Xu, Sensitive simultaneous determination of catechol and hydroquinone using a gold electrode modified with carbon nanofibers and gold nanoparticles, Microchim. Acta 173 (2011) 119–125.

[51] C. Wang, R. Yuan, Y. Chai, F. Hu, Simultaneous determination of hydroquinone, catechol, resorcinol and nitrite using gold nanoparticles loaded on poly-3-amino-5-mercapto-1, 2, 4-triazole-MWNTs film modified electrode, Anal. Methods 4 (6) (2012) 1626–1628.

[52] S. Erogul, S.Z. Bas, M. Ozmen, S. Yildiz, A new electrochemical sensor based on Fe3O4 functionalized graphene oxide-gold nanoparticle composite film for simultaneous determination of catechol and hydroquinone, Electrochim. Acta 186 (2015) 302–313.

[53] L. Zheng, L. Xiong, Y. Li, J. Xu, X. Kang, Z. Zou, J. Xia, Facile preparation of polydopamine-reduced graphene oxide nanocomposite and its electrochemical application in simultaneous determination of hydroquinone and catechol, Sens. Actuators B 177 (2013) 344–349.

[54] M.A. Al-Azzawi, R.W. Saleh, Fabrication of environmental monitoring amperometric biosensor based on alkaloids compound derived from catharanthus roseus extract nanoparticles for detection of cadmium pollution of water, Chem. Methodol. 7 (5) (2023) 358–371, https://doi.org/10.22034/chemm.2023.380792.1643.

[55] S. Pour Karim, R. Ahmadi, M. Yousefi, K. Kalateh, G. Zarei, Interaction of graphene with amoxicillin antibiotic by in silico study, Chem. Methodol. 6 (11) (2022) 861–871, https://doi.org/10.22034/chemm.2022.347571.1560.

[56] M.T. Vardini, N. Abbasi, A. Kaviani, M. Ahmadi, E. Karimi, Graphite electrode potentiometric sensor modified by surface imprinted silica gel to measure valproic acid, Chem. Methodol. 6 (5) (2022) 398–408, https://doi.org/10.22034/chemm.2022.328620.1437.
[57] B. Fazeli-Nasab, L. Shahraki-Mojahed, Z. Beigomi, M. Beigomi, A. Pahlavan, Rapid detection methods of pesticides residues in vegetable foods, Chem. Methodol. 6 (1) (2022) 24–40, https://doi.org/10.22034/chemm.2022.1.3.
[58] O. Abdulrahman Hamad, R. Kareem, P. Khdir Omer, Recent developments in synthesize, properties, characterization, and application of phthalocyanine and metal phthalocyanine, J. Chem. Rev. 6 (1) (2024) 39–75, https://doi.org/10.48309/jcr.2024.412899.1250.
[59] M. Manuel, A. Jennifer, A review on starch and cellulose-enhanced superabsorbent hydrogel, J. Chem. Rev. 5 (2) (2023) 183–203, https://doi.org/10.22034/jcr.2023.382452.1209.
[60] M.S. Hasan, M.R. Sardar, A. Shafin, M.S. Rahman, M. Mahmud, M.M. Hossen, A brief review on applications of lignin, J. Chem. Rev. 5 (1) (2023) 56–82, https://doi.org/10.22034/jcr.2023.359861.1186.
[61] J. López-Dino, J. Hernández-Paz, I. Olivas-Armendáriz, C. Rodríguez González, Structural design of biosensor: a review, J. Med. Pharmaceut. Chem. Res. 5 (10) (2023) 915–934, https://doi.org/10.48309/jmpcr.2023.177586.
[62] T. Gholami, Investigating the effect of metacognitive therapy and cognitive behavioral therapy on anxiety and depression of single middle-aged men, Int. J. Adv. Stud. Human. Soc. Sci. 12 (3) (2023) 214–221, https://doi.org/10.22034/ijashss.2023.381596.1129.
[63] Z. Dourandish, F. Garkani Nejad, R. Zaimbashi, S. Tajik, M.B. Askari, P. Salarizadeh, S.Z. Mohammadi, H. Oloumi, F. Mousazadeh, M. Baghayeri, H. Beitollai, Recent advances in electrochemical sensing of anticancer drug doxorubicin: a mini-review, Chem. Methodol. 8 (4) (2024) 293–315, https://doi.org/10.48309/chemm.2024.441220.1761.
[64] S. Javame, M. Ghods, Analysis of K-Banhatti polynomials and calculation of some degree based indices using (a, b)-Nirmala index in molecular graph and line graph of TUC4C8(S) nanotube, Chem. Methodol. 7 (3) (2023) 237–247, https://doi.org/10.22034/chemm.2023.366592.1620.
[65] N. Farhami, A computational study of thiophene adsorption on boron nitride nanotube, J. Appl. Organometal. Chem. 2 (3) (2022) 148–157, https://doi.org/10.22034/jaoc.2022.154821.
[66] Z.H. Mahmoud, Y. Ajaj, A.M. Hussein, H.N.K. Al-Salman, M.A. Mustafa, E. H. Kadhum, E. Kianfar, CdIn2Se4@ chitosan heterojunction nanocomposite with ultrahigh photocatalytic activity under sunlight driven photodegradation of organic pollutants, Int. J. Biol. Macromol. 267 (2024) 131465.
[67] H.N.K. Al-Salman, C.Y. Hsu, Z.N. Jawad, Z.H. Mahmoud, F. Mohammed, A. Saud, E. Kianfar, Graphene oxide-based biosensors for detection of lung cancer: a review, Results Chem. 101300 (2023).
[68] D. Bokov, A. Turki Jalil, S. Chupradit, W. Suksatan, M. Javed Ansari, I.H. Shewael, E. Kianfar, Nanomaterial by sol-gel method: synthesis and application, Adv. Mater. Sci. Eng. 2021 (2021) 1–21.
[69] A. Mirani, E. Kianfar, L. Maleknia, M. Javanbakht, Recent advances in nicotine electrochemical biosensors: a review, Case Stud. Chem. Environ. Eng. 100753 (2024).